Algorithm Theoretical Basis Document (ATBD) for the Conical-Scanning Microwave Imager/Sounder (CMIS) Environmental Data Records (EDRs)

Volume 1: Overview
Part 1: Integration

Version 1.1 – 15 March 2001

Solicitation No. F04701-01-R-0500

Submitted by:
Atmospheric and Environmental Research, Inc.
131 Hartwell Avenue
Lexington, MA 02421-3126

With contributions by:
Jean-Luc Moncet, Sid Boukabara, Alan Lipton, John Galantowicz,
Hélène Rieu-Isaacs, Ned Snell, Jennifer Hegarty, Xu Liu, Ernesto Sendoya

Prepared for:
Boeing Satellite Systems
919 Imperial Avenue
El Segundo, CA 90245

AER Document P757-TR-I-ATBD-OVERVIEW-INT-20010315

REVISION HISTORY

Version	Release Date	POC	Comments
1.0	10/2000	J. L. Moncet, AER, Inc.	First Draft Version
1.1	3/2001	J. L. Moncet, AER, Inc.	Extensive changes in content and formatting for first official release (virtually every section updated)

RELATED CMIS DOCUMENTATION

Government Documents

Title	Version	Authorship	Date
CMIS SRD for NPOESS Spacecraft and Sensors	3.0	Associate Directorate for Acquisition NPOESS IPO	2 March 2001

Boeing Satellite Systems Documents

Title		Covering
ATBD for the CMIS TDR/SDR Algorithms		
ATBD for the CMIS EDRs	**Volume 1: Overview**	**Part 1: Integration**
		Part 2: Spatial Data Processing • Footprint Matching and Interpolation • Gridding • Imagery EDR
	Volume 2: Core Physical Inversion Module	
	Volume 3: Water Vapor EDRs	Atmospheric Vertical Moisture Profile EDR Precipitable Water EDR
	Volume 4: Atmospheric Vertical Temperature Profile EDR	
	Volume 5: Precipitation Type and Rate EDR	
	Volume 6: Pressure Profile EDR	
	Volume 7: Cloud EDRs	Part 1: Cloud Ice Water Path EDR
		Part 2: Cloud Liquid Water EDR
		Part 3: Cloud Base Height EDR
	Volume 8: Total Water Content EDR	
	Volume 9: Soil Moisture EDR	
	Volume 10: Snow Cover/Depth EDR	
	Volume 11: Vegetation/Surface Type EDR	
	Volume 12: Ice EDRs	Sea Ice Age and Sea Ice Edge Motion EDR Fresh Water Ice EDR
	Volume 13: Surface Temperature EDRs	Land Surface Temperature EDR Ice Surface Temperature EDR
	Volume 14: Ocean EDR Algorithm Suite	Sea Surface Temperature EDR Sea Surface Wind Speed/Direction EDR Surface Wind Stress EDR
	Volume 15: Test and Validation	All EDRs

Bold = this document

TABLE OF CONTENTS FOR VOLUME 1, PART 1

LIST OF TABLES

LIST OF FIGURES

1. Introduction

The algorithm theoretical basis document (ATBD) provides the underlying mathematical and theoretical background and documentation for the integration of the EDR (Environmental Data Record) algorithms for the Conical Microwave Imaging Sounder (CMIS) developed by Atmospheric and Environmental Research, Inc. (AER) in support of the National Polar-orbiting Operational Environmental Satellite System (NPOESS). The objective of the ATBD is to facilitate an understanding of our approach to the CMIS retrieval problem from a phenomenological perspective in the context of the current state-of-the-art. The overview contained in this document provides the rationale for our integration concept and to demonstrate its performances. The individual EDR algorithms are described in detail in the individual CMIS EDR (Environmental Data Record) ATBDs. Table 1 provides a road map to visualize the overall integration. The centerpiece of our approach is the Core Physical Inversion Algorithm (the "core module") designed to simultaneously retrieve temperature and water vapor profiles along the sensor view path, cloud liquid water (CLW), cloud top pressure, skin temperature and surface emissivity. The requirement which drives the design of the core module is the extraction of water vapor profiles from the CMIS measurements. The approach we have selected is best suited for producing water vapor retrievals in clear and cloudy conditions (both liquid water and cirrus ice) and over all surface types, therefore maximizing the range of conditions over which the related EDRs (Atmospheric Vertical Moisture Profile (AVMP), Precipitable Water (PW), Total Water Content (TWC)) will be made available). The integration ATBD shows the integration of all of the EDR algorithms in the optimal way to produce the integrated CMIS EDR algorithm.

Table 1: Structure of the ATBD for the CMIS EDRs.

Title	Covering
Volume 1: Overview	**Part 1: Integration**
	Part 2: Spatial Data Processing • Footprint Matching and Interpolation • Gridding • Imagery EDR
Volume 2: Core Physical Inversion Module	
Volume 3: Water Vapor EDRs	Atmospheric Vertical Moisture Profile EDR Precipitable Water EDR
Volume 4: Atmospheric Vertical Temperature Profile EDR	
Volume 5: Precipitation Type and Rate EDR	
Volume 6: Pressure Profile EDR	
Volume 7: Cloud EDRs	Part 1: Cloud Ice Water Path EDR
	Part 2: Cloud Liquid Water EDR
	Part 3: Cloud Base Height EDR
Volume 8: Total Water Content EDR	
Volume 9: Soil Moisture EDR	
Volume 10: Snow Cover/Depth EDR	
Volume 11: Vegetation/Surface Type EDR	
Volume 12: Ice EDRs	Sea Ice Age and Sea Ice Edge Motion EDR Fresh Water Ice EDR
Volume 13: Surface Temperature EDRs	Land Surface Temperature EDR Ice Surface Temperature EDR
Volume 14: Ocean EDR Algorithm Suite	Sea Surface Temperature EDR Sea Surface Wind Speed/Direction EDR Surface Wind Stress EDR
Volume 15: Test and Validation	All EDRs

Bold = this document

2. Overview of the CMIS Instrument Characteristics

The baseline CMIS instrument is a conical-scanning microwave radiometer consisting of channels from 6.9 GHz to 183 GHz. There are options to extend the spectral coverage to 340 GHz to enhance ice cloud detection. The CMIS instrument is a dual reflector system. A 2.2 m diameter antenna provides spatial resolution ranging from 68 km to 15 km at 6.9 GHz and 89 GHz, respectively. A second smaller antenna is used for the frequencies above 89 GHz. CMIS has window channels, the frequencies chosen to avoid atmospheric absorption lines, around 6, 10, 19, 37, and 88 GHz and atmospheric sounding channels around 23, 50-60, 60, 166, and 183 GHz. The instrument rotates continuously at 31.6 rpm on an axis perpendicular to the ground taking observations along nearly semi-circular arcs centered on the satellite ground track. Successive arcs scanned by a single sensor channel are separated by about 12.5 km along-track (depending on satellite altitude.) Calibration data is collected from a source (hot) and deep-space reflector (cold) viewed during the non-earth-viewing portion of the rotation cycle. Each observation (or sample) requires a finite sensor integration time which also transforms the sensor instantaneous field of view (IFOV), the projection, or footprint, of the antenna gain pattern on the earth, into an observation effective field of view (EFOV). The start of each sample is separated by the sample time which is slightly longer than the integration time. The sample time is t_s = 1.2659 ms for all channels with the exception of 10 GHz (exactly $2t_s$) and 6.8 GHz ($4t_s$). All samples fall on one of three main-reflector scan-arcs or a single secondary-reflector scan arc (166 and 183 GHz channels families only).

Table 2: CMIS baseline channel configuration.

Channel Name	RF Center Frequency (GHz)	Polarization	RF 3 dB Passband (MHz)
6V, 6H	6.625	V, H	350
10V, 10H	10.65	V, H	100
10R, 10L	10.65	RC, LC	100
18V, 18H	18.7	V, H	200
18P, 18M	18.7	45°, -45°	200
18R, 18L	18.7	RC, LC	200
23V, 23H	23.8	V, H	400
36V, 36H	36.5	V, H	1000
36P, 36 M	36.5	45°, -45°	1000
60VA	50.300	V	134
60VB	52.240	V	1280
60VC	53.570	V	960
60VD	54.380	V	440
60VE	54.905	V	350
60VF	55.490	V	340
60VG	56.660	V	300
60VJ	59.380	V	280
60VK	59.940	V	440
60LL	60.3712	LC	57.6
60LM	60.4080	LC	16.0
60LU	60.4202	LC	8.4
60LV	60.5088	LC	44.8
60L FFT (1-5)	varies	LC	1.00
60L FFT (6-10)	varies	LC	0.50
60L FFT (11-30)	varies	LC	0.25
60L FFT (31-35)	varies	LC	0.50
60L FFT (36-40)	varies	LC	1.00
89V	89.0	V	4000
89H	89.0	H	4000
166V	166.0 ± 0.7875	V	3000
183VA	183.31 ± 0.7125	V	1275 ea
183VB	183.31 ± 3.1	V	3500 ea
183VC	183.31 ± 7.7	V	4500 ea

3. EDR Algorithm Products

3.1. List of EDRs with Priorities

The CMIS instrument collects global microwave radiometry and sounding data to produce microwave imagery and other meteorological and oceanographic data. It is the primary instrument for satisfying all the EDRs listed in Table 3 with their priorities.

Table 3: CMIS EDRs with Priorities.

Priority	EDR
1A	Atmospheric Vertical Moisture Profile
1A	Soil Moisture
1A	Sea Surface Winds Speed
2A	Sea Surface Winds Direction
2A	Sea Surface Temperature
2A	Precipitable Water
2A	Atmospheric Vertical Temperature Profile
2A	Cloud Liquid Water
2A	Cloud Ice Water Path
2A	Total Water Content
2A	Precipitation (Type, Rate)
2B	Land Surface Temperature
2B	Ice Surface Temperature
2B	Sea Ice Age and Sea Ice Edge Motion
3A	Snow Depth
3B	Snow Cover
3B	Surface Wind Stress
3B	Pressure Profile
3B	Cloud Base Height
3B	Fresh Water Ice
3B	Vegetation /Surface Type
3B	Imagery

3.2. EDR Requirements Summary

The NPOESS requirements for the CMIS EDRs are summarized in Table 4. In addition to these program requirements, our algorithm design is based on the following set of criteria:

EDR Performance: Our CMIS EDR algorithm is designed to meet all of the EDR requirements, including the algorithm timing requirements. The algorithms will perform properly in wide range of global conditions with the efficiency of a 1-D approach.

Robustness: Our CMIS algorithms are designed and tested over the widest range of environmental conditions, including stressful situations such as the retrieval of snow over coastline. The algorithms are designed to handle situations considered to be anomalous by minimizing the reliance on climatological correlations.

Maturity and Risk: The selected algorithms have operational heritage and/or research if such heritage exists and satisfies the SRD requirements. The heritage algorithms are extended where significant performance enhancement can be obtained with low risk. Because CMIS imposes requirements more demanding than the previous microwave sensors the approach proposed for processing the CMIS SDR product contains several unique enhancing features compared to current operational SSM/I processing algorithms.

Quality Control Capability and Confidence Level: Our CMIS algorithms contain various quality control criteria to ensure that situations for which the performance is degraded beyond nominal performance, or for which no report is possible, are detected and flagged. A confidence level for the quality of the EDR product is critical information to most users and is part of the EDR definition. To this end and under normal conditions of operation, it is necessary to ensure that derived EDRs are consistent with the measurements from which they have been derived.

Flexibility and Potential for Growth: Our modular software structure provides the flexibility to configure the algorithm to produce all or part of the CMIS EDRs or change the spatial resolution of an EDR in order to adapt to different hardware environments. This modular structure also facilitates future technology insertion.

Graceful Degradation: Our approach addresses operational considerations such as the graceful degradation of EDR performance in case of a loss of channels. That is, the algorithm will continue to operate when data from one or more CMIS channels is missing, though the EDR performance may degrade.

Other Sensors Independency: Our CMIS EDR algorithm continues to operate when auxiliary data and/or data from other sensors is unavailable. This is true for both external information from other NPOESS sensors (e.g., VIIRS) and for data from other sources (e.g., NWP model output). That is, the algorithm is configured to use auxiliary data when available to enhance performance beyond standalone performance, and no change in the algorithm is required when the auxiliary data is unavailable.

Table 4: Summary of EDR Requirements.

EDR	Horizontal Cell Size (km)	Threshold Performance	Measurement Range
Atmospheric Vertical Moisture Profile	15	Clear Surface to 600 mb — 20 % or 0.2 g/kg 600 mb to 300 mb — 35 % or 0.1 g/kg 300 mb to 100 mb — 35 % or 0.04 g/kg Cloudy Surface to 600 mb — 20 % or 0.2 g/kg 600 mb to 300 mb — 40 % or 0.1 g/kg 300 mb to 100 mb — 40 % or 0.04 g/kg	0 - 30 g/kg
Soil Moisture	40	10%	0 - 100%
Sea Surface Winds Speed	20	2 m/s or 20% of true value, whichever is greater	3 - 25 m/s
Sea Surface Winds Direction	20	20 deg for wind speeds greater than 5 m/s 20 deg for wind speeds from 3 - 5 m/s	0 - 360 deg
Sea Surface Temperature	50	0.5 K	271 K - 313 K
Precipitable Water	25	Greater of 10% or 2mm	0 - 75 mm
Atmospheric Vertical Temperature Profile	Surface to 20 mb — 40 20 to 0.01 mb — 200	Clear Surface to 700 mb — 1.6 K/1 km layers 700 mb to 300 mb — 1.5 K/1 km layers 300 mb to 30 mb — 1.5 K/3 km layers 30 mb to 1 mb — 1.5 K/5 km layers 1 mb to 0.01 mb — 3.5 K/5 km layers Cloudy Surface to 700 mb — 2.5 K/1 km layers 700 mb to 300 mb — 1.5 K/1 km layers 300 mb to 30 mb — 1.5 K/3 km layers 30 mb to 1 mb — 1.5 K/5 km layer 1 mb to 0.01mb — 3.5 K/5 km layers	180 K - 335 K
Cloud Liquid Water	20	Over ocean: 0.25 kg/m^2 Over land: 0.5 kg/m^2	0 - 5 kg/m^2
Cloud Ice Water Path	50	10% or 5 g/m^2	0 - 2.6 kg/m^2
Total Water Content	20	Point Measurement: 2 kg/m^2 Global Average: 1 kg/m^2	0 - 200 kg/m^2
Precipitation (Type, Rate)	15	Rate: 2 mm/hr	Rate: 0 – 50 mm/hr Type: Rain and Ice
Land Surface Temperature	50	2.5 K	213 K – 343 K
Ice Surface Temperature	30	1 K	213 K – 293 K (ice surface)
Sea Ice Age and Sea Ice Edge Motion	20	Probability of Correct Typing (Ice Age) 70% Measurement Uncertainty (Ice Motion): 1 km/day	Age: Ice Age Classes first year, multi-year Motion: 0 - 50 km/day
Snow Depth	12.5	20 % (snow/no snow)	Snow Depth Ranges: > 0 cm (Any Snow Thickness) Measurement range 0-100%
Surface Wind Stress	50	7 km	Consistent with SSW
Pressure Profile	25	0 - 10 km: 5% 10 - 30 km: 10%	10 - 1050 mb
Cloud Base Height	25	2 km	0 - 15 km
Fresh Water Ice	20	Ice Edge boundary: 10 km Ice Concentration: 20% or 1/10	1/10 to 10/10 concentration

EDR	Horizontal Cell Size (km)	Threshold Performance	Measurement Range
Vegetation /Surface Type		Correct Typing Probability: 70%	8 types in CMIS classification
Imagery	Global	Derived	Dynamic range of all measurement channels

3.3. Accuracy and precision metrics

Throughout all volumes of this ATBD, specification and evaluation of accuracy and precision metrics follow the customary procedures for environmental measurements. That is, accuracy describes the measurement bias and precision describes the measurement standard error regardless of the source of the error (e.g., instrument, algorithm, environment) and without stratification (except as noted). We point this out because the SRD requirements definitions are written as if precision covers only measurement errors in an idealized situation where each measurement in the statistical ensemble occurs under identical environmental conditions. A specification of this type is unverifiable with real-world data where conditions are never identical for any two observations. In addition, for many EDRs with precision metrics, the SRD-required precision is smaller than the corresponding accuracy. This is inconsistent with the fact that for environmental measurements accuracy can be minimized by algorithm calibration whereas precision cannot. We reconcile the requirements ambiguity by switching the SRD numeric values for accuracy and precision wherever the accuracy metric is greater. The modified requirements are marked with an asterisk—Measurement Precision* and Measurement Accuracy*—wherever they appear in all volumes of the ATBD. Table 5 summarizes our revised requirements.

Table 5: Summary of switched measurement accuracy and precision requirement values

EDR	Measurement Accuracy*	Measurement Precision*
Sea Surface Winds Speed	1 m/s	2 m/s or 20% of true value, whichever is greater
Sea Surface Winds Direction	10 deg	20 deg or W > 5 m/s. 20 deg (TBR) for W from 3-5 m/s
Precipitable Water	1 mm	Greater of 10 % or 2 mm
Cloud Ice Water Path	5 %	10 % or 5 g/m^2 (TBR)
Precipitation (Rate)	1 mm/hr	2 mm/hr
Land Surface Temperature	0.5 K	2.5 K

4. Approach Overview

The baseline CMIS algorithm contains the three stages of processing shown in Figure 1. The first stage consists of footprint matching and other spatial processing of the SDRs. The second stage involves the retrieval of geophysical parameters. Finally, post-processing is done to produce the final EDR output. These steps are detailed in the following sections.

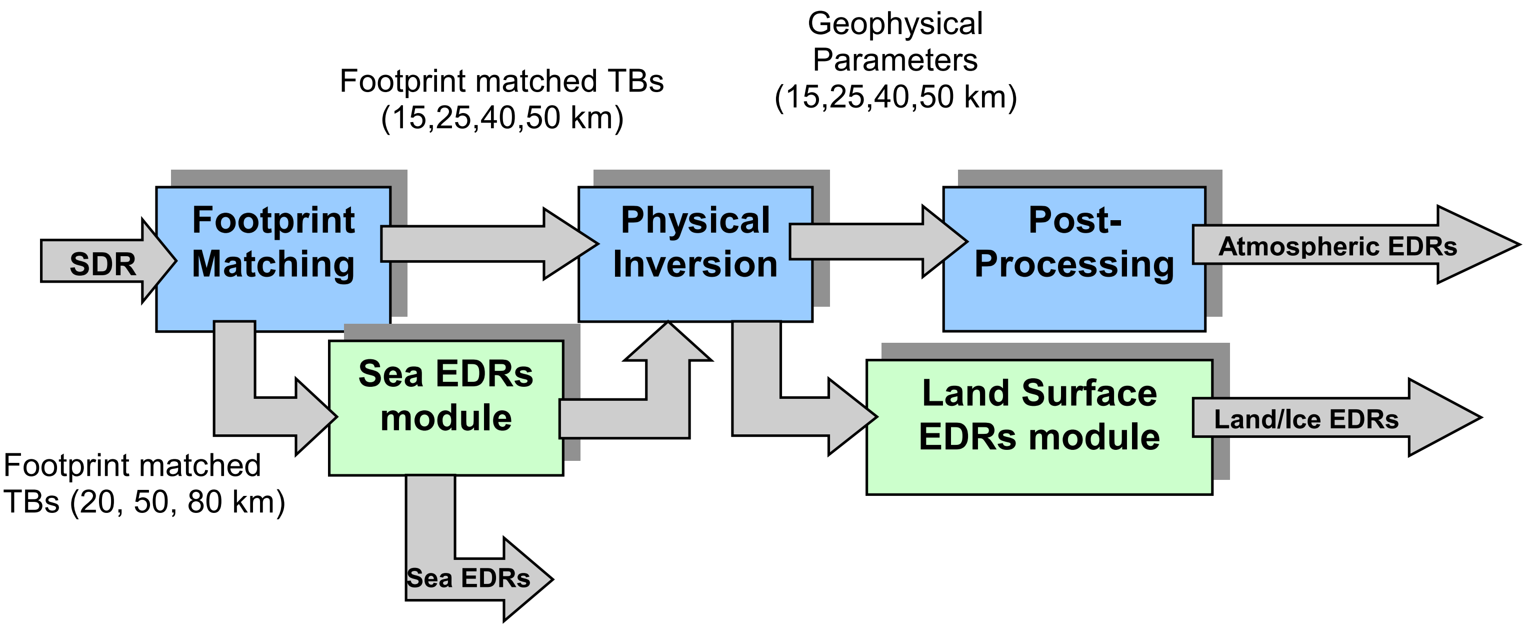

Figure 1: High Level Diagram of Algorithm Integration.

4.1. Spatial Processing

The reporting of CMIS EDRs is required at various horizontal resolutions ranging from 200 km to 15 km. Each EDR is derived from measurements at multiple frequencies. Because of the disparity in the footprint size of the different channels, some spatial processing is required to ensure that all of the channels used in the EDR derivation sense the same atmospheric volume and surface area. This is accomplished using an optimal filtering technique to re-map the neighboring footprints corresponding to a specific channel onto a target antenna pattern scaled to the desired resolution. The same target is used for all channels for a given EDR. More details about this spatial processing may be found in the ATBD for CMIS EDR Algorithms Overview - Part 2: Footprint Matching and Interpolation.

4.2. General Retrieval Approach

EDRs are divided into four categories: Ocean Surface EDRs, Sounding EDRs, Land/Ice Surface EDRs, and Precipitation EDRs. The general retrieval approaches are slightly different for each category and are discussed in the following sections.

4.2.1. Ocean Surface EDRs

The ocean module incorporates proven algorithms for the Sea Surface Temperature, Surface Wind Speed, and Surface Wind Stress EDRs. State-of-the-art science for passive radiometry was used to develop the Wind Direction algorithm. All of the details about the ocean EDR algorithms are given in the *ATBD for CMIS EDRs Vol. 14: Ocean EDR Algorithm Suite*, prepared by Remote Sensing Systems, Inc.

Table 6: Ocean EDRs ATBD.

ATBD Title	Author
Ocean EDR Algorithm Suite	RSS, Inc.

4.2.2. Sounding EDRs

The baseline algorithm selection for the sounding EDRs for non-precipitating conditions is a non-linear physical inversion approach. In the following text, and other ATBDs, this is referred to as the Core Physical Retrieval Module (or Core Module, described in details in the Core Module ATBD). Heritage algorithms for this technique include those of Eyre [Eyre, 1989a and 1989b], and the AMSU algorithm for AIRS [AIRS-Team, 1999]. A variational approach of this algorithm is operational at the ECMWF (European Center for Medium-Range Weather Forecasting). This algorithm produces atmospheric profiles of temperature and water vapor, cloud liquid water (CLW) and cloud ice parameters as well as surface emissivity and temperature (so-called geophysical parameters) from the CMIS observations. These geophysical parameters are transformed into the desired EDRs by post-processing (Section 4.3). The retrieval under precipitating conditions is described in Section 4.2.4.

The choice of a physical retrieval approach for the CMIS sounding EDRs addresses the strict performance requirements for the water vapor profile EDR (a critical CMIS EDR). This approach maximizes the range of conditions under which these requirements will be met, including cloudy atmospheres and retrievals over land. It also minimizes the impact of cloud liquid water on the atmospheric temperature retrievals. Further, the physical retrieval approach also addresses the extension of performance to land surfaces for related water vapor products (Precipitable Water (PW), Total Water Content (TWC)) and the optimization of vertical temperature profile performance in cloudy conditions.

Because the microwave radiances at the top of the atmosphere are sensitive to the characteristics of the cloud and surface properties, cloud/surface parameters must be derived simultaneously with water vapor and temperature profiles in order to meet the requirements for the related EDRs. Cloud parameters available from the core module retrieval are used in the derivation of CLW, TWC, CIWP (Cloud Ice Water Path) as well as cloud base height (CBH). The surface skin temperature and spectral emissivity obtained as a by-product of the physical inversion are exploited in the derivation of land surface EDRs wherever there is proven performance benefit over heritage algorithms.

Several other important attributes of the core module include:

- Geophysical parameters are treated in a physically and radiometrically consistent manner
- Provides a framework for easy incorporation of external constraints into the retrieval system (e.g. data from models and/or other NPOESS sensors).
- Provides a mechanism for interface with NWP data assimilation
- Approach is robust with respect to anomalous conditions because the physical constraints alleviate the need to train the algorithm for all possible situations, *a priori* decisions are minimized, and there is an inherent quality control capability
- Approach designed for graceful degradation by inherently handling the loss of channels or external data

All of the details about the Core physical Inversion algorithm and the sounding EDR algorithms are given the ATBDs listed in Table 7.

Table 7: Sounding EDRs ATBDs.

ATBD Title	Author
Core Physical Inversion Module	AER, Inc.
Water Vapor EDRs	AER, Inc.
Atmospheric Vertical Temperature Profile EDR	AER, Inc.
Pressure Profile EDR	AER, Inc.
Cloud EDRs – Part 1: Cloud Ice Water Path EDR	AER, Inc.
Cloud EDRs – Part 2: Cloud Liquid Water EDR	AER, Inc.
Cloud EDRs – Part 3: Cloud Base Height EDR	AER, Inc.
Total Water Content EDR	AER, Inc.

4.2.3. Land Surface EDRs

The approach for the land surface EDRs draws on heritage algorithms. CMIS enhancements include pre-removal of atmospheric "contamination" through use of the core module product (Section 4.2.2). Innovative methods are applied to snow cover and VST retrievals. All of the details about the land surface EDR algorithms are given in the ATBDs listed in Table 8.

Table 8: Land Surface and Ice EDRs ATBDs.

ATBD Title	Author
Soil Moisture EDR	AER, Inc.
Snow Cover/Depth EDR	AER, Inc.
Vegetation/Surface Type EDR	AER, Inc.
Ice EDRs	AER, Inc.
Surface Temperature EDRs	AER, Inc.

4.2.4. Precipitation

The precipitation module consists of proven algorithms to exploit spatial information in a 2-dimensional retrieval approach resulting in the use of multi-spectral and multi-spatial measurements to derive precipitation type and rate. Under precipitating conditions the module treats ice water path (IWP), liquid water path (LWP), consisting of cloud liquid water (CLW) and rain water in the precipitating clouds, and total water content (TWC). Details about the precipitation algorithm are given in the Precipitation ATBD (see Table 9).

Table 9: Precipitation EDR ATBD.

ATBD Title	Authors
Precipitation Type and Rate	G. Petty (Univ. Wisconsin) AER, Inc.

Figure 2 provides more specific information about the ocean and land precipitation modules. In summary, the core module has the ability to detect and flag cases that possibly contain precipitation. For ocean scenes a refined precipitation mask based on the scattering index is computed and used by the rain algorithm. Strict quality control at the core module level ensures that no precipitation will be found outside of "possible precipitation" masks. Simultaneously, depending on the output of the core module quality control, the ice water path is computed. This is also used by the rain algorithm. A similar process occurs for land scenes, with the exception of the rain mask refinement. The important feature of this algorithm is that there is an inter-consistency between the rain rate, ice water path, and liquid water path. Thus there is an overall consistency in the derived total water content. The types of quality control flags referenced in the figure are given in Table 10 and are discussed in more detail in the Core Module ATBD (ATBD Volume 2).

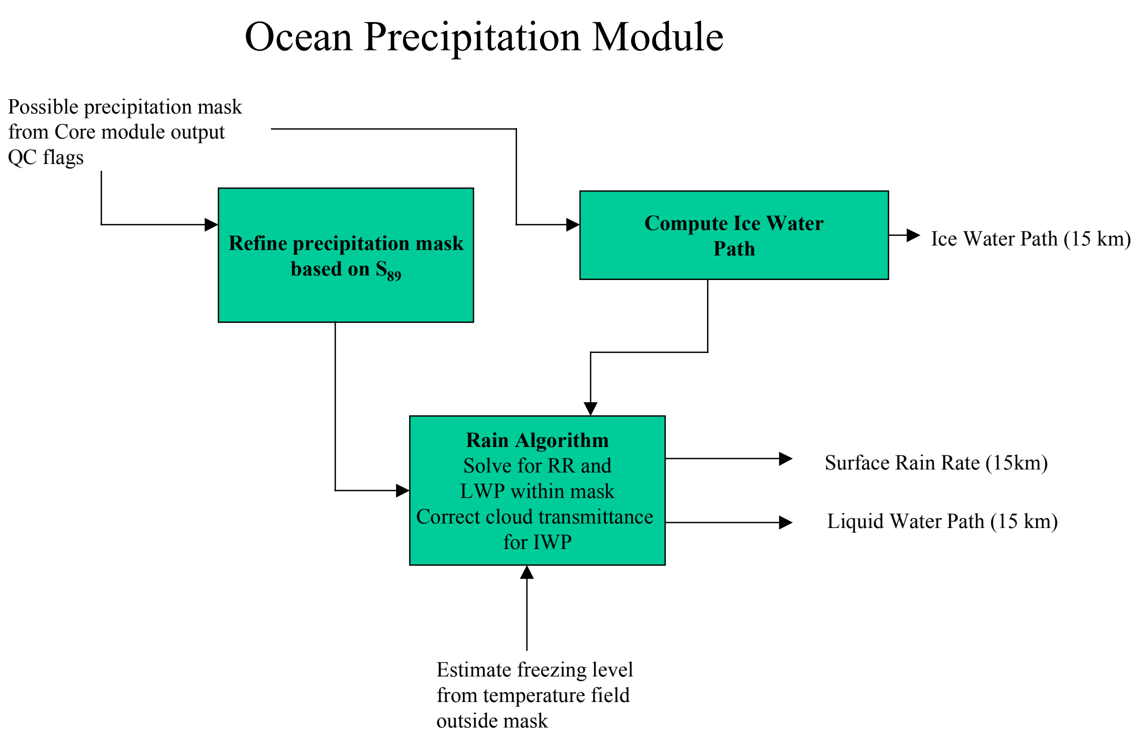

(a)

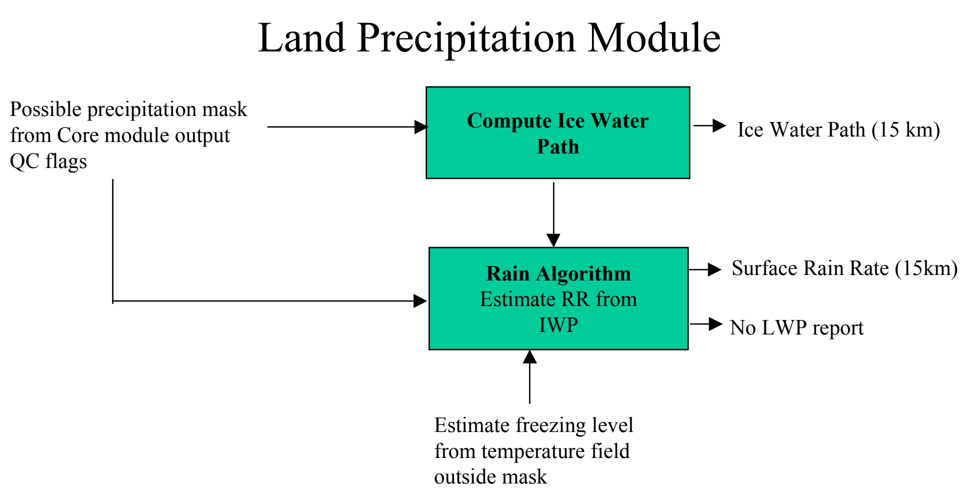

(b)

Figure 2: Detail of ocean and land precipitation modules. Note that the ice water path computation occurs only if the conditions in Table 10 are met.

Table 10: Core module output quality control flags. Shaded areas indicate conditions for which the ice water path is computed; the "*" indicates conditions for which VIIRS data could be used (if available) to check the cloud top location.

Convergence Status	LF+HF (no scattering)	LF+HF (scattering)	LF only (no moisture profile or IWP available)
1	No precipitation; No detectable ice	No precipitation; Ice present	No precipitation; Check temperature field for ice
2	Possible rain; No ice	Possible rain; Thin ice clouds	Possible rain; Thin ice clouds
3	N/A	Ice impacts low frequency channels* or rain is present	Ice impacts low frequency channels* or rain is present

4.3. Post-Processing

Post-processing is required to map the sounding retrievals to the vertical and horizontal spatial grids specified by the EDR requirements. Profile parameters generated by the core physical inversion module are produced on the 40 level vertical grid used by the radiative transfer model in the sensor coordinate system. Post-processing vertically re-samples the profile to meet vertical reporting-interval requirements. In addition, a horizontal re-mapping stage is added to produce vertical profiles. Other sounding products are derived from the vertically re-mapped temperature and water vapor profiles. These EDRs are, pressure profile, precipitable water, total water content. The EDR generation processes and corresponding post-processing tasks are given in Table 11.

Table 11: EDR generation process and post-processing task.

EDR Class	EDR	Main Module	Main Module Output	Post-Processing
Sounding	AVMP	Core Module (15 km)	Moisture Profile	Vertical re-mapping; Interpolate to reporting levels
	AVTP	UA Module	Mesospheric Temperature	Vertical re-mapping; Merge upper and lower
		Core Module (40 km)	Temperature Profile	
	PP	Core Module (25 km)	Temperature & Moisture Profiles; Psfc	Vertical re-mapping of temperature/moisture; Pressure computation
	PW	Core Module (25 km)	Moisture Profile; Psfc	Vertical integration of water vapor mixing ratio
	LWP (no precip)	Core Module (20 km)	LWP	
	IWP (no precip)	Core Module (50 km)	IWP	
	TWC (no precip)	Core Module (20 km)	Moisture & Temperature Profile; LWP, IWP, Cloud Top/Base; Psfc	Compute TWC in 3 km layers
Ocean Surface	SST	SST Module	SST	
	Wind Speed	Wind Speed Module (20 km)	Wind Speed	
	Wind Direction	Wind Speed (50 km); Wind Direction Module	Wind Direction; Wind Speed	Ambiguity removal
	Wind Stress	Wind Speed (20 km)	Wind Speed	Compute wind stress
Land	Soil Moisture	Soil Moisture Module	Soil Moisture	
	LST	Core Module (40 km)	Surface Temperature	Re-gridding of Tb to fix Earth grid
	IST	Core Module (20 km)	Surface Temperature	Re-gridding of Tb to fix Earth grid
	Sea Ice Age & Motion	Sea Ice Module	Sea Ice Age, Concentration, Edge Location, and Edge Motion	
	Fresh Water Ice	Fresh Water Ice Module	Fresh Water Ice	
	Snow Cover and Depth	Snow Module	Snow Cover	
	VST	VST Module	VST	
Precipitation	Precipitation Type & Rate	Precipitation Module	Precipitation Type & Rate	
	LWP (under precip)	Precipitation Module	LWP	Match to 20 km resolution
	IWP (under precip)	Precipitation Module	IWP	Match to 50 km resolution
	TWC (under precip)	Precipitation Module	TWC	Match to 20 km resolution

5. Algorithm Integration

5.1. Radiometric Consistency

The algorithm concept for the sounding EDRs (Section 4.2.2) is extended to all of the CMIS EDRs wherever it benefits the performance. This ensures that consistency is maintained between all of the EDRs and the observations. Figure 3 illustrates how EDRs are related to geophysical parameters. The relationship is key to ensuring that estimates of the EDRs produced by the CMIS EDR algorithm are inter-consistent and consistent with the radiometric data from CMIS or other sensor used in the processing.

The CMIS measurements are directly related to the geophysical parameters through the radiative transfer equation as:

$$T_{Bi} = F\big(T(P); q(P); \varepsilon_{sfc}; Tskin; CLW; IceParam\big) \qquad (1)$$

where T_{Bi} is the brightness temperature measured in each channel i.

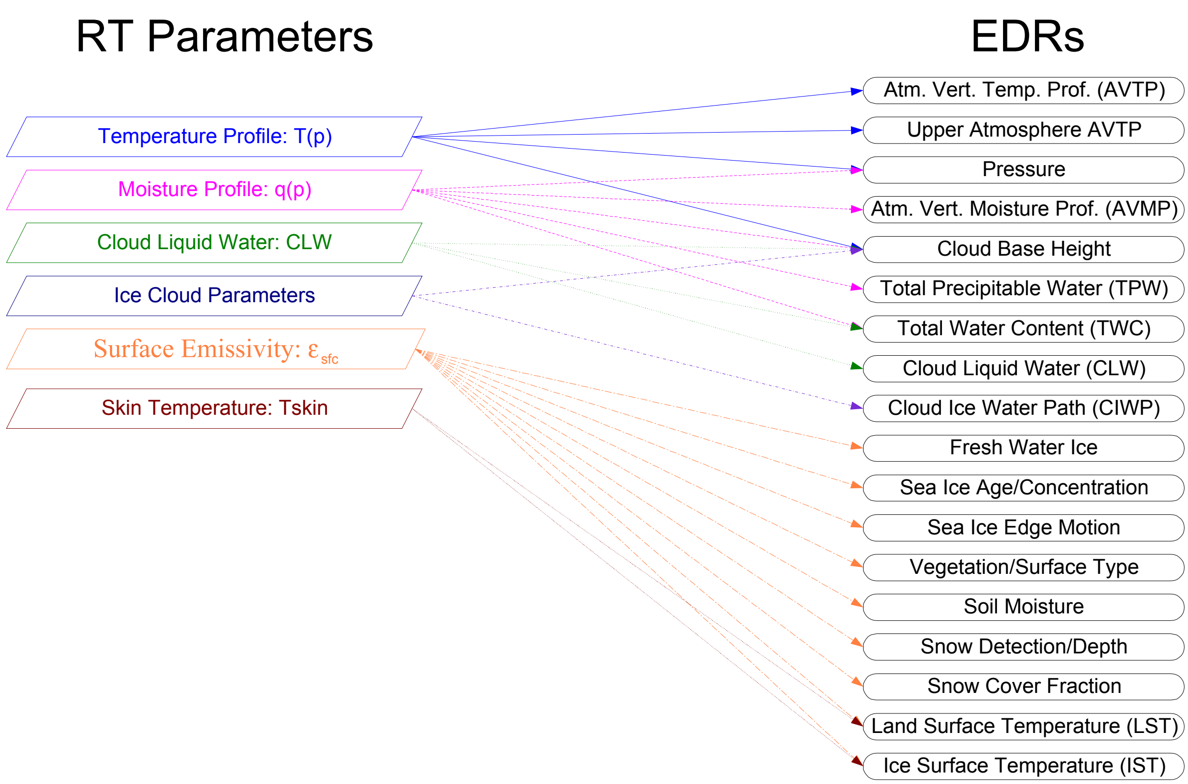

Figure 3: Relationship between geophysical parameters and the CMIS EDRs.

Our algorithm system assures that each EDR can be processed independently from the overall system. For example, as shown in Table 11, the precipitable water (PP) sounding EDR may be obtained by using the core module at 25 km resolution if processing power is limited. However, if all of the EDRs are to be processed, the cascade approach (Section 5.3) will maintain radiometric consistency among EDRs and between similar products at different spatial resolutions. That is, if all reported EDRs at a particular location are used in a radiative transfer model, the computed brightness temperatures will agree with the observations. This design also facilitates data interpretation, data fusion and data assimilation by exploiting an integrated architecture while eliminating redundant processes in EDR production. Overall this integrated processing scheme will provide enhanced performance and quality control capabilities at reduced computational cost (see Section 7) for the land and ice EDRs, the precipitation EDRs, and for the sounding EDRs at high spatial resolution.

Additional factors must be considered in the design of the integrated algorithm system. These are outlined in Table 12. For the land/ice surface EDRs the surface emissivity and temperature derived from the physical algorithm may be exploited wherever there is a proven performance benefit over heritage approaches that use (atmospheric contaminated) brightness temperatures as direct input. For the precipitation EDRs the quality control flags from the core module may be used as a “possible precipitation” mask, while knowledge of environmental conditions in proximity to precipitating scenes enhances the characterization of precipitation. Finally, the multi-spatial-scale processing of the cascade architecture links processes at different spatial resolutions, ensuring consistency between the core module output at different scales without the computational drawbacks of a full 3-dimensional approach. This “cascade” design allows for the best mix of vertical and horizontal resolution for the profile EDRs by using low spatial-resolution solution to constrain higher spatial-resolution retrievals, thus enhancing the high resolution sounding performance. Further, the use of a first-guess from the low resolution retrieval accelerates the high-resolution algorithm convergence. This approach is shown schematically in Figure 4, and discussed in Section 5.3.

Table 12: List of integration attributes. Shaded areas indicate core module output.

Spatial Resolution	EDR	Core Physical Inversion Required	Integration Attributes
80 km	SST		
50 km	Wind direction		SST from SST Module
	CIWP	Globally	
	LST	(Better emissivity / Tskin separation)	Obtained as a by-product with no computational cost
40 km	AVTP	Cloudy	
	Soil Moisture		LST estimate from core module; 20 km resolution surface type information; Reduced atmosphere/surface cross-talk
25 km	Cloud Base Height	(Priority III)	
	Pressure Profile	(Priority III)	
	PW	Land/Snow/Ice	
	IST	(Better emissivity / Tskin separation)	Obtained as a by-product with no computational cost
20 km	Wind Speed		
	Wind Stress		
	VST	(Priority III)	
	Fresh Water Ice		Reduced atmosphere/surface cross-talk
	Sea Ice		Reduced atmosphere/surface cross-talk
	CLW	Land (objectives)	
	TWC	Non-precipitating conditions	
15 km	AVMP	Globally	18/23 GHz contribute to estimate; Enhanced horizontal/vertical resolution
	Precipitation		Core module products provide mask, estimate of freezing level, cloud top/base, water phase, surface type
	Snow Cover/Depth		Precipitation flag from precipitation module

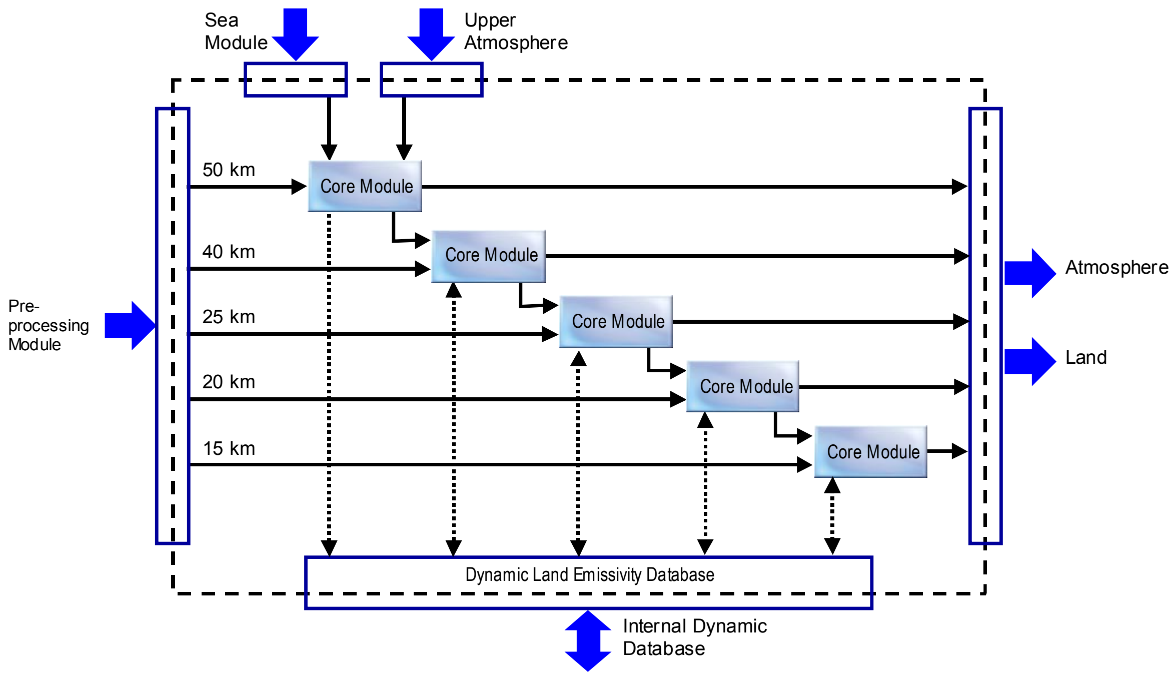

Figure 4: Schematic illustration of the cascade retrieval approach.

5.2. Overall Functional Flow Diagram

Figure 5 shows a top level diagram of the integration design we chose for the CMIS EDR algorithms. It is to be read as a timeline from left to right. A core physical inversion module utilizing a "cascade" design (Section 5.3) links the EDR modules and provides consistency among EDRs that have different cell sizes. As discussed in Section 4.2.2, the Core Module (shown in the cyan boxes) is a non-linear physical inversion algorithm which simultaneously retrieves atmospheric temperature, water vapor, cloud water, surface temperature and emissivity. Purple shadowed boxes refer to algorithm modules that operate on multiple cells (e.g., vertical re-mapping of sounding product). Dashed lines refer to potential links for dynamic databases. Our overall integration design enables the use of a single set of calibrated, corrected SDR data to feed all EDR algorithms in coordination with a set of common databases across EDRs for static geophysical parameters such as terrain type and altitude.

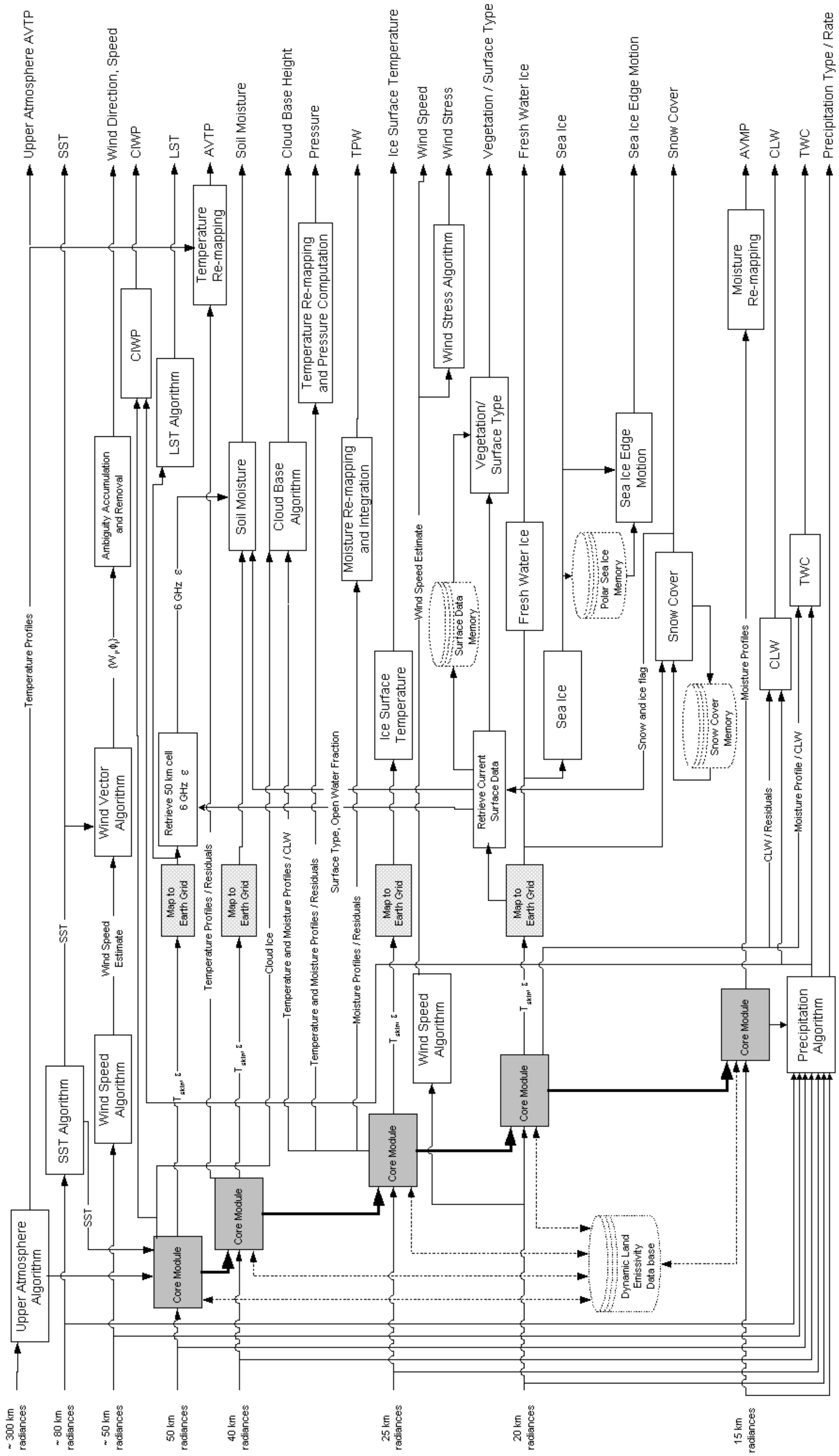

Figure 5: Top level flow diagram of the integrated CMIS EDR algorithm.

5.3. The Cascade Concept

5.3.1. Introduction to the Cascade Algorithm

For each CMIS channel noise level of the interpolated radiance will increase as the cell size decreases from 50 km to 12.5 km. Therefore, it is expected that the retrieval performance will be worse for small cell sizes. For some low frequency channels such as 6.9, 10.8 and 19 GHz, the footprint size of the measurements is large. Consequently the interpolated radiances to small cell sizes will have so much noise that it is no longer beneficial to include them in the retrieval. Excluding these low frequency channels will result in a degradation in the retrieved surface parameters such as surface temperature and surface emissivity, which in turn will degrade the performance of cloud and moisture retrievals. Also, for inhomogeneous scenes the low frequency channels may bring in contradicting information due to the fact the original footprints are not Nyquest-sampled.

There are various ways to perform retrievals for different EDRs (such as moisture profiles and TPW) using radiances obtained at different cell sizes. A basic method would consist of performing retrieval individually for each cell size and reporting the corresponding EDRs for that cell size. It has the advantage of being simple and straightforward. The retrieved parameters from other cell sizes can be used as initial guess for the current cell size. Another way is to adopt a cascade approach, which takes advantages of the information from larger cell sizes. The cascade algorithm will perform retrieval for the largest cell size first and use the retrieval product intelligently for smaller cell sizes. The cascade algorithm uses information from all the frequencies at all cell sizes in an optimal way. We have adopted the cascade approach.

5.3.2. Physical Basis of the Cascade Algorithm

As mentioned above, the information from all the frequencies at all cell sizes should be used in the retrieval when the cell size becomes smaller. The cascade approach uses *a priori* information obtained from the larger cell size retrieval as constraint for the small cell-size retrieval. This takes advantage of the low noise channels from the large cell sizes and the solution will be weighted significantly towards the retrieval results from the larger cell size retrievals if the scene is close to homogeneous. Under homogeneous conditions there is no need to perform retrieval for small cell sizes. However, under inhomogeneous conditions the retrieval constraints need to be adjusted to account for the variation of the retrieved parameters, but the retrieval will converge rapidly since both the constraint and the initial guess are close to the solution.

5.3.3. Description of the Cascade Algorithm

The cascade algorithm involves an initial retrieval at 50 km resolution, a test of scene inhomogeneity, and quality control. The three step process is outlined below.

5.3.3.1 Cascade Step 1: Retrieval at 50 km

The cascade algorithm begins by performing a retrieval for the largest cell size (50 km) using the unified retrieval method described in the Core Module ATBD. The EDR corresponding to the current cell size is reported. Along with the retrieval parameters, a covariance matrix corresponding to the retrieved parameters is saved for use as a constraint in the cascade algorithm. The covariance carries information from larger cell size into the smaller cell size retrievals. The calculated CMIS radiances for the current cell size are also kept in the next step. The covariance matrix is calculated according to the equation:

$$S = S_x - S_x K^T \left(K S_x K^T + Sy \right)^{-1} K S_x \tag{1}$$

where x is the state vector containing retrieval parameters, S_x is the error covariance matrix associated with *a priori* state vector, y represents the radiance vector, S_y is the error covariance matrix associated with y, and K is the Jacobian matrix.

5.3.3.2 Cascade Step 2: Test of Scene Inhomogeneity

The CMIS radiances calculated at 50 km spatial resolution are used to test the inhomogeneity of the scene. These radiances are compared with the measured radiances from the next cell size. If the radiance difference is less than the NEdT, the scene is homogeneous and no retrieval is necessary for the next cell size. Otherwise, the scene is inhomogeneous and the covariance matrix obtained from last retrieval is relaxed. The retrieved parameters from larger cell size are used both as initial guess and *a priori* information (background).

Since clouds are most likely to be the cause of the inhomogeneity, the correlation between cloud parameters (cloud height, base and amount) and other state parameters is removed from the *a priori* covariance matrix. The variances of the cloud parameters themselves are relaxed to the values used in the non-cascade algorithm while the cloud amount initial guess and background is set to zero. Because the moisture profile has a small-scale variability, its correlation with other parameters is removed, and the variance of the moisture profile is relaxed by 40% taking into account typical moisture variations. Similarly, the variances for temperature, surface emissivity and surface temperature should also be relaxed empirically to account for possible inhomogeneity. (Detailed studies will be performed to quantify the extent of this relaxation). A constrained physical inversion is then performed.

5.3.3.3 Cascade Step 3: Quality Control

Quality control is performed to assess the success/failure of retrievals. The chi-squared radiance residuals are used as one of the quality control indicators. If the inhomogeneity is large, the constraint from last cell size retrieval may be too strong and the chi-squared value may be much larger than the number of channels used in the retrieval. This indicates that the retrieval should be repeated with either a more relaxed constraint, or a baseline physical retrieval constrained with a climatology covariance matrix.

Another quality control indicator that will be utilized is the spatial correlation of the retrieved parameters. For example, if the difference in the moisture profiles between large and small cell sizes is larger than what is physically reasonable, the retrieval should be rejected or repeated with the baseline physical retrieval with a climatology constraint.

The cascade process continues until all the cell sizes are processed. A flow chart describing the cascade algorithm is shown in Figure 6.

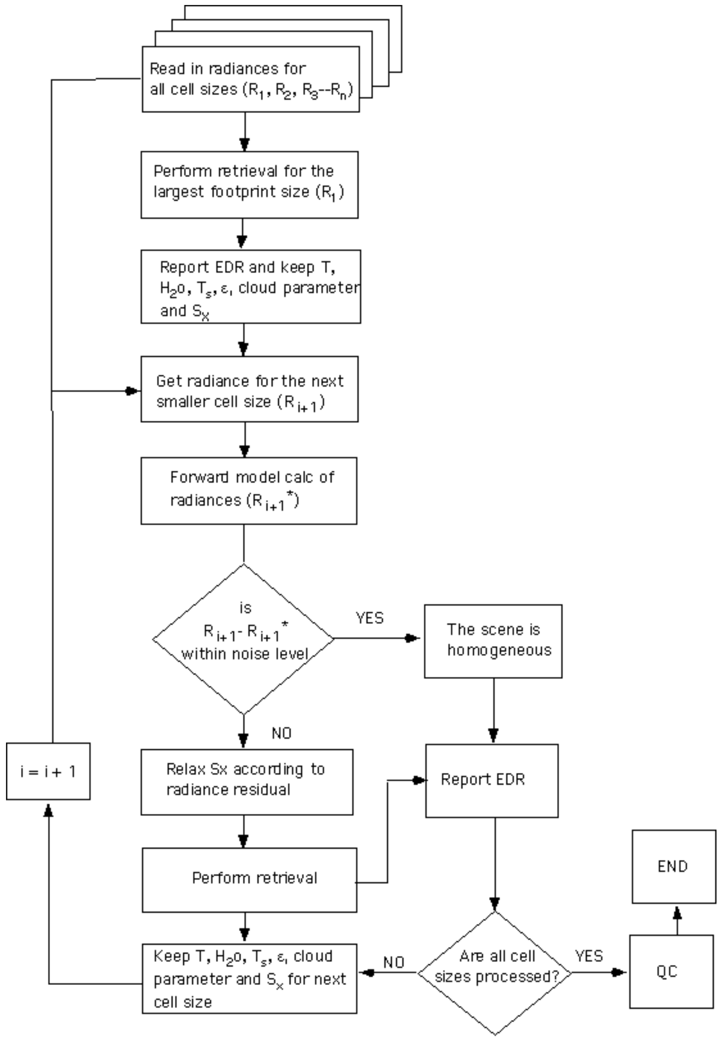

Figure 6: Flow diagram for the cascade algorithm.

5.3.4. Cascade Validation Under Inhomogeneous Cloudy And Moisture Field Condition

5.3.4.1 Scene Description

Scene 1: Two cell sizes are used, one at 50 km and one at 15 km. The scene is homogeneous except for the cloud and the moisture fields**:** the 50 km cell has 20% more cloud and 10% less moisture than the 15 km cell. These conditions are illustrated in Figure 7. The simulation is performed using 200 global ocean profiles, with random variations in cloud amount, height and cloud liquid water on a 50 km grid in the simulations.

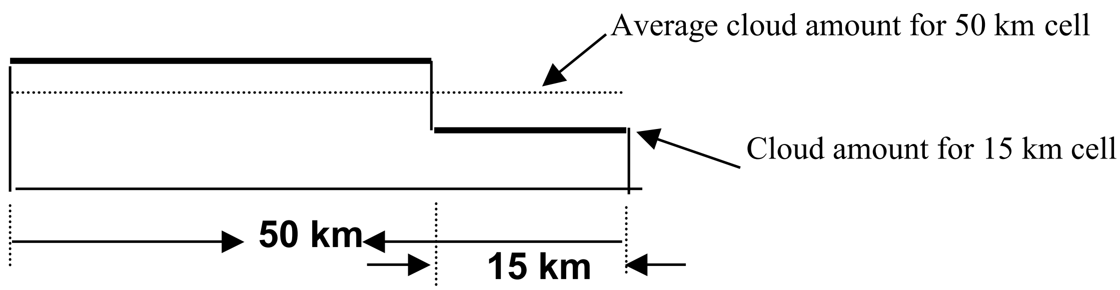

Figure 7: Illustration of the inhomogeneous scene used in the cascade validation.

Scene 2: The conditions are the same as *Scene 1* but the cloud liquid amount in 15 km cell used in the simulation is independent of that in the 50 km cell, and the cloud liquid water amount varies randomly between 0 and 0.5 mm.

5.3.4.2 Retrieval Results

The temperature and moisture profile retrieval results from *Scene 1* are shown in Figure 8. These results indicate that the cascade algorithm provides almost 50 km cell accuracy on the 15 km reporting cell. The temperature and water vapor errors are shown with and without the cascade. The black-solid lines are the results from the 50 km cell size constrained by climatology while the purple-dotted lines are the temperature and moisture results for the 15 km cell constrained using the 50 km cell size retrieval results. The blue-dashed lines are the retrieval results from 15 km cell size without using cascade scheme (i.e. the constraints are from climatology).

Table 13 shows the Cloud Liquid Water (CLW) and Surface Temperature ($T_{surface}$) retrieval performances. The results from *Scene 2* are shown in Figure 9 and Table 14. Even for this extreme situation, the cascade scheme delivers nearly 50 km accuracy on a 15 km reporting grid.

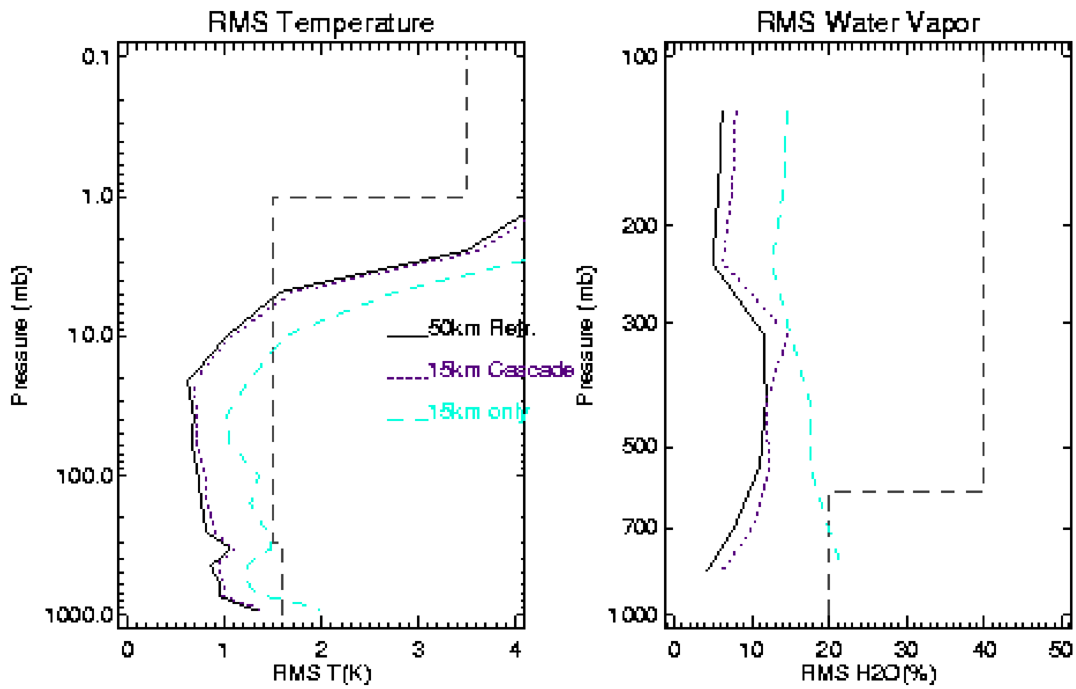

Figure 8: Retrieval results for *Scene 1*: Temperature and water vapor retrieval performance under inhomogeneous conditions.

Table 13: Retrieval results from *Scene 1*: Cloud Liquid Water (CLW) and Surface Temperature ($T_{surface}$) retrieval performance under inhomogeneous conditions.

	No Cascade	With Cascade
CLW rms error	0.09 kg/m^2	0.02 kg/m^2
$T_{surface}$ rms error	2.9 K	1.0 K

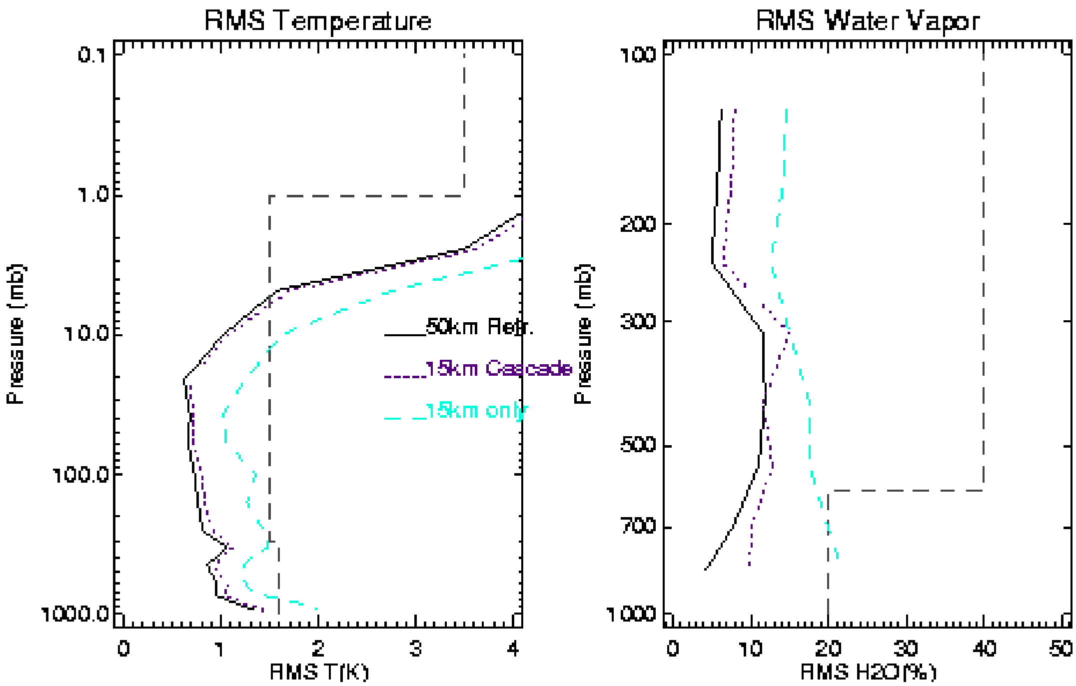

Figure 9: Retrieval results for *Scene 2*: Temperature and water vapor retrieval performance under inhomogeneous conditions.

Table 14: Retrieval results from *Scene 2*: Cloud Liquid Water (CLW) and Surface Temperature ($T_{surface}$) retrieval performance under inhomogeneous conditions.

	No Cascade	With Cascade
CLW rms error	0.09 kg/m^2	0.04 kg/m^2
$T_{surface}$ rms error	2.9 K	1.0 K

While the profile retrievals shown above illustrate the retrieval differences with and without the cascade approach, a more illustrative simulation is to compare the retrieval of 2-dimensional water vapor fields. These simulations are shown in Figure 10. Part “a” shows the true water vapor field used in the simulation. The 50 km and 15 km retrievals are shown in parts “b” and “c”. The 50 km retrieval is able to reproduce the gross vertical structure of the profile, but there is some smoothing along the frontal boundary where the change in water vapor occurs on a spatial scale of less than 50 km. With the 15 km retrieval there is again a fairly reasonable retrieval of the vertical structure, but for this case the sensor noise has increased, leading to apparently lower resolution in the retrieved field. (This can also be seen in the retrieval simulations of Figure 8 and Figure 9). Finally, part “d” shows the 15 km cascade retrieval. It is clear that the cascade approach provides a substantial improvement over the direct retrieval approach as the retrieval is able to capture the finer structure of the water vapor which occurs around the frontal boundary.

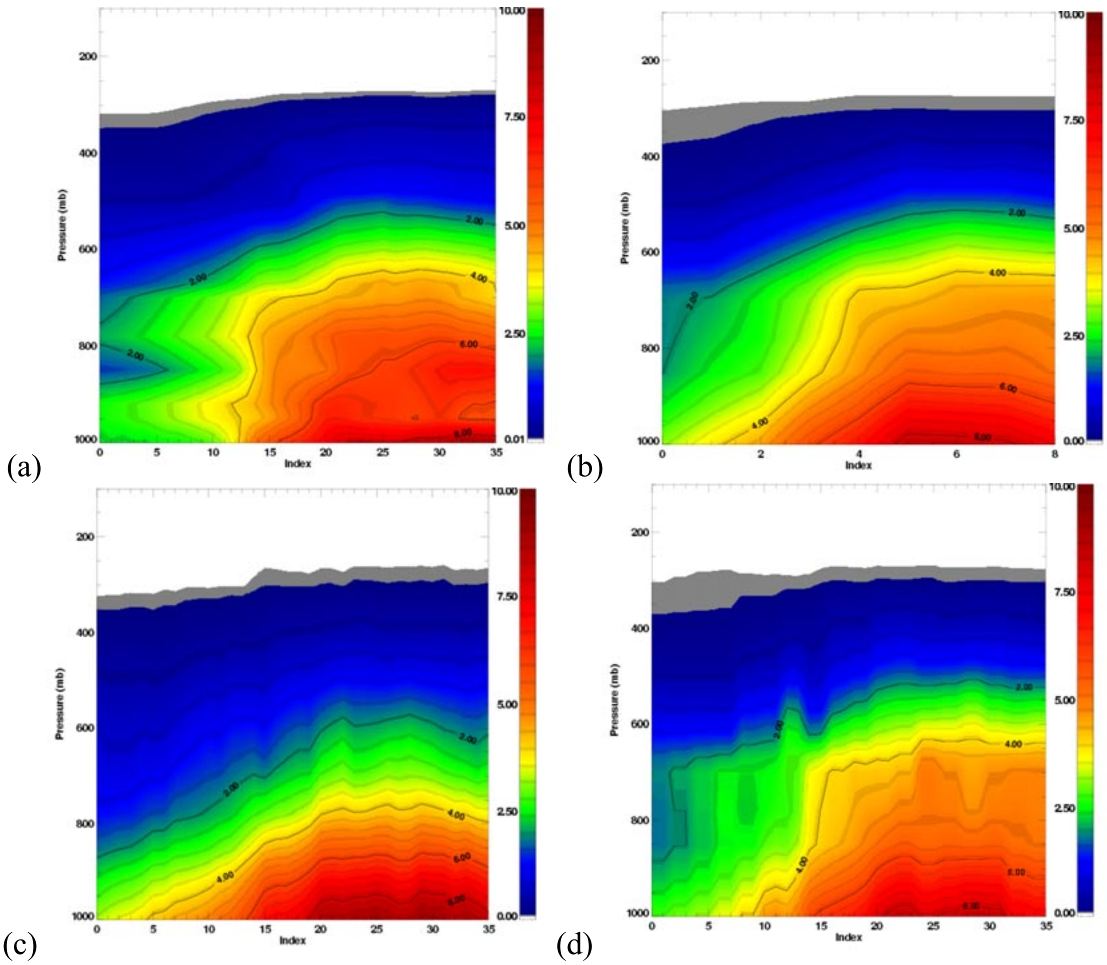

Figure 10: Comparison of cascade and non-cascade water vapor retrievals: (a) True water vapor field; (b) 50 km retrieval; (c) 15 km retrieval without cascade; (d) 15 km retrieval with cascade.

5.3.5. Cascade Retrieval Approach Conclusions

The cascade design (emphasized in Figure 5 with the cascade of Core Modules) ensures radiometric consistency between the various EDRs and between similar products at different spatial resolutions. In other words, the various surface/atmospheric output products generated by the CMIS EDR algorithms, when fed into a radiative transfer model, produce radiances that match the input measurements.

This cascade design also provides a computationally efficient algorithm that meets the requirements for convertibility to an operational algorithm. The use of lower resolution products as a constraint for the higher resolution retrievals reduces the number of iterations in the retrieval process. The algorithm also adapts itself naturally to the degree of spatial inhomogeneity in a scene. In spatially homogeneous atmospheres, the low resolution product is already consistent with the higher resolution SDRs (the modeled radiances are within expected noise level), i.e., no additional iteration is required. When additional iterations are required, channel selection can be used to minimize the number of channels and state vector dimensions. For instance, the atmospheric temperature profile is updated at 15 km resolution only if significant variations occur within nominal 40 km cell.

6. Software Implementation

6.1. Core Process Definition

The proposed parallel architecture for the Core Module(s) is shown schematically in Figure 11. The current Core Module(s) will be replaced by a process containing a Core Module Coordinator/Thread controller, an interpolation processor, a scalable buffer, and *N* Core Retrieval processes.

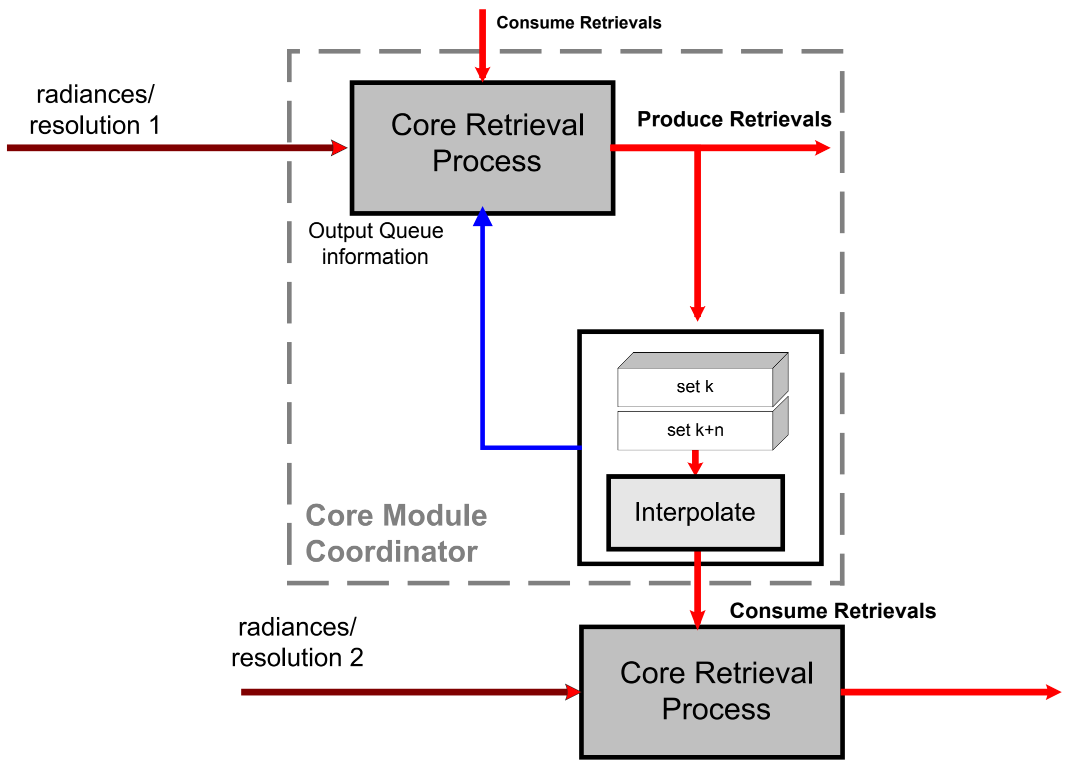

Figure 11: Core Process Implementation.

6.2. Parallel Process Implementation

The Core process (shown in Figure 11) manages multiple retrieval tasks (threads) given the allocated computational resources. The thread controller manages retrieval threads based on a priority scheme (data availability and down stream process status) and interpolates and fills scalable output buffer. The Core Retrieval thread continually processes gridded/interpolated data located in the process input buffer.

7. Timing Estimates

The NPOESS requirements state that the algorithm must process 1.25 orbits of data: (4000 scan lines or 3,376,000 cells) in 20 minutes. The results of our preliminary timing study show a total of 664.5 minutes, decomposed as shown in Table 15. Sea Ice Edge Motion was considered to be a separate process and is not included in these calculations. A 32 CPU server @ 200MHz meets the 20 minute requirement. The requirements are also met on the current following technologies: Sun Microsystems Ultra 80 16x450 MHz, IBM RS6000 S80 16x450 MHz and Beowulf (Linux) cluster. These results show that our design approach is low risk, and that there is still room for future extension of the CMIS EDR processing concepts (e.g. 3-D spatial processing or the implementation of cloud multiple scattering). Table 16 shows estimates of timing for the Core Physical Retrieval Algorithm for all cell sizes that appear in the CMIS Sensor Requirements Document. The 30 km and 15 km cell sizes have been eliminated from the processing scheme. The 30 km cell is for the IST EDR, which is now reported at 15 km, while the 15 km cell is for the Snow Cover Depth EDR, which is now reported at 20 km. A discussion of the details of these differences may be found in the relevant ATBD.

Table 15: Decomposition of the Total EDR Algorithm Timing

	Footprint Matching/Interpolation	Core Module 50, 40, 25, 20, 15 km	Map to Earth grid	EDR level 2,3
CPU Minutes, SGI 195 MHz	6.5 s	615 s	23 s	<20 s

Table 16: Core Physical Retrieval Module Timing, including a ratio of the processing time to the 20 minute NPOESS processing time requirement.

Cell Size (km)	Number of Footprints	Processing Time (minutes)	Ratio to 20 min Processing Time
50	176000	22.386	1.1193
40	466374	116.59	5.8297
30	621832	0	0
25	704000	134.32	6.7158
20	880000	167.89	8.3947
15	1176000	174.11	8.7057
12.5	7461990	0	0
Total	3376000	615.3	30.765

APPENDIX A: Co-registration Error Analysis

EDR retrieval errors can be caused by errors in the spatial coregistration of the channels used in the retrieval. This error source was evaluated by considering several types of scene spatial structure that could cause brightness temperatures in a misregistered channel to be different from a correctly registered channel. We chose to consider spatial structure characteristics that can have short spatial scales in nature and can have a substantial impact on retrieval performance. The parameters considered were cloud liquid, surface emissivity, and surface temperature.

The impact of co-registration errors was considered band-by-band. The procedure will be described first for the case where cloud liquid water is the scene parameter with spatial structure. CMIS brightness temperatures were simulated for a set of scenes. For one band, the cloud liquid water was set to a value different from all the other bands. The amount of difference was varied. Retrievals were performed and the impact on performance for several EDRs was tracked as a function of the cloud liquid difference. For each EDR, a threshold was set on the amount of performance degradation that could be tolerated relative to the performance obtained when the cloud liquid difference was zero. That performance impact threshold could then be identified with a certain cloud liquid water difference.

The next step was to identify a certain cloud liquid water difference with a co-registration error, measured in distance. We considered the case where the spatial structure in the cloud liquid water field was a step function between two areas with uniform cloud liquid water, and we assumed that each field of view straddled the location where the step function occurred. We further assumed that the field-of-view (FOV) consisted of a uniformly weighted circle. This is a relatively extreme case. A misregistration in the direction perpendicular to the step function causes the misregistered channel to "see" a scene with different FOV-average cloud liquid, and the difference is related to the magnitude of the step and the distance of misregistration. The magnitude of the cloud liquid water step was set to 0.1 kg/m^2. A given cloud liquid difference could thus be related to a misregistration distance. A similar process was followed for surface temperature, where the step was assumed to be 15 K.

For surface emissivity, the spatial contrast was between two surface types. The nominal type was a mean emissivity spectrum for barren land, for which the emissivities are relatively low. It was assumed that the nominal FOV was entirely over barren land. The FOV was assumed to be immediately adjacent to a densely vegetated region (step function change) where the emissivity is high (0.985 for V polarization and 0.960 for H polarization). A misregistered channel had a portion of its FOV crossing over the surface type boundary and thus its FOV-average emissivity would be higher than it would be without misregistration. It was further assumed that 33% of the scenes would have such contrasts, which is a stressing assumption.

Table 17 and Table 18 list the misregistration errors that could be tolerated for each considered EDR without causing the EDR retrieval error to amplify beyond its assigned threshold of misregistration-induced error. For each of the EDRs, the misregistration requirements were evaluated for each of the relevant types of scene structure (inhomogeneity). For some EDRs retrievals were considered over different surfaces that can have a significant impact on retrieval performance (land and ocean). The overall requirement for each channel is derived from the minimum over all the EDRs and types of structure.

Table 17: Misregistration errors which may be tolerated for each moisture EDR, where the shaded values indicate the design drivers.

	Inhomogeneity:	Cloud	sfc emis	SST	Cloud	sfc emis	SST	Cloud	sfc emis	SST
	EDR:	AVMP	AVMP	AVMP	PW	PW	PW	CLW	CLW	CLW
	Sfc type	ocean	land	ocean	ocean	land	ocean	ocean	land	ocean
Band	Misregistration req									
6	1.4	15	15	8	25	25	14	20	20	11
10	1.4	15	15	8	25	25	14	20	20	11
18	1.1	2.3	1.2	2.8	3.9	1.2	2.7	1.1	5	2.3
23	1.9	2.9	2.1	2.8	10	1.9	2	2.7	2.5	7
36	1.3	1.3	1.6	7	2.1	1.8	4.5	1.8	5	5
50	2.9	2.9	4	4.5	2.9	3.6	4.5	5	20	5
89	1.1	1.25	15	4.5	1.9	25	6	1.1	20	3.5
166	7	7	15	8	15	25	14	10	20	11
183	2.3	2.3	15	8	6	25	14	3.5	20	11

Driver

Table 18: Misregistration errors which may be tolerated for each temperature EDR, where the shaded values indicate the design drivers.

	Inhomogeneity:	Cloud	sfc emis	SST	Cloud	SST	sfc emis
	EDR:	AVTP	AVTP	AVTP	SST	SST	LST
	Sfc type	ocean	land	ocean			
Band	Misregistration req						
6	1.4	7	9	7	7	1.4	6
10	1.4	7	9	7	7	1.4	6
18	1.1	2.5	2.7	4	2.3	3	3.2
23	1.9	4.5	2.7	4	4.7	2.3	3.2
36	1.3	3.1	40	4	1.5	5.5	14
50	2.9	6	40	7	9	23	8
89	1.1	3.1	40	3.3	3	3.5	50
166	7	7	40	22	7	18	50
183	2.3	7	40	22	9	28	50

APPENDIX B: Temporal Registration

There are two aspects of the CMIS design that raise questions regarding temporal registration: CMIS has a two-reflector antenna design, where the channels with frequencies at 89 GHz and below are on the main, large reflector and the higher frequencies are on the secondary reflector. The reflectors are oriented in opposite azimuth angles around the spin axis, so there is at least on half rotation of the antenna between views of a given spot on the Earth from the low and high frequency channels.

The channels on the main reflector do not all have a common Earth incidence (zenith) angle (EIA). The EIA offsets are such that the antenna rotates nine times between the views of a point along track by the channels with the largest and smallest EIA.

Temporal variations of CMIS EDR phenomenology are not significant on time and space scales represented by the CMIS antenna. The time for 180° rotation of antenna (the interval between the nearest views of the two reflectors) is 0.95 s. The interval between the first and last large-reflector feed to scan a spot on the sub-satellite track is 17.1 s. Meteorological phenomena at these time scales have space scales (< 20 m) much smaller than CMIS cell sizes (Orlanski, I., 1975: A rational subdivision of scales for atmospheric processes. *Bull. Amer. Meteorol. Soc.*, **56**, 527-530). For example, an atmospheric frontal boundary that is spatially large enough to be represented in a CMIS EDR (about 15 km) would typically move at less than 4 meters per second. An reasonable upper limit for frontal motion would be 20 meters per second, which corresponds to movement of about 20 meters between the views of the two reflectors and less than 0.4 km between the first and last views of the channels on the large reflector. These displacements are negligible in relation to the CMIS horizontal cell sizes, the smallest of which is 15 km.

APPENDIX C: Calibration Accuracy Requirements

The radiometric data on which the EDR retrieval algorithms operate are the empirically corrected brightness temperature (ECTB) data discussed in the ATBD for Temperature Data Records and Sensor Data Records. The ECTBs differ from the SDRs to the extent that corrections have been applied to adjust for any systematic differences between the SDRs and brightness temperatures computed by applying the CMIS radiative transfer model to collocated ground-truth geophysical data. Those differences arise from any systematic sensor calibration errors and systematic errors in the radiative transfer model that cannot be attributed to a particular source and explicitly corrected. The empirical correction process removes a large proportion of the systematic differences, leaving the ECTBs with relatively small residual calibration errors.

EDR performance was evaluated against the residual calibration errors. For each of the EDRs a portion of the error budget was allocated to each the absolute ECTB accuracy and the relative accuracy, as discussed in the ATBD volumes for the individual EDRs. Simulations were performed by adding absolute or interchannel biases at the ECTB level to determine the magnitude of the error at the ECTB level that corresponded to the EDR budgeted error.

For the absolute accuracy evaluation, bias tolerances were computed as applied to all channels simultaneously and for each band separately. The absolute accuracy requirement for a band was taken as the larger of the bias tolerance for the band by itself and the tolerance for all bands together.

For the interchannel accuracy evaluation, we tested biases of opposite sign applied to pairs of bands or pairs of channels. The pairs tested were those for which interchannel biases were considered to be a possible driver on EDR performance. The absolute accuracy requirements place a limit on the interchannel accuracy, such that the interchannel accuracy for a pair cannot be any larger than the sum of the absolute accuracy requirements of the two that make up the pair. Therefore, interchannel accuracy requirements need to be specified only where the required value is smaller than that sum.

For ocean EDRs, the accuracy requirements were evaluated using all-channel biases and with randomly assigned interchannel biases. This procedure did not attribute the interchannel accuracy requirements to individual pairs of bands and channels, so the actual pair-by-pair requirements are not as stringent as the results of this evaluation method indicate.

The residual absolute and interchannel accuracy requirements are in Table 19 and Table 20, respectively. For some EDRs, retrievals were considered over different surfaces that can have a significant impact on retrieval performance (land and ocean). The overall requirement for each channel is derived from the minimum over all the EDRs and types of surface. In Table 19, a value of 9 is given wherever the value was 9 or larger (and thus not a driver). For Table 20, any value 1.8 or larger is not precise but simply indicates that the value is 1.8 or larger.

Table 19: Absolute accuracy by EDR and summarized.

Band	Abs acc reqt	AVMP ocean	AVMP land	AVMP ice	PW ocean	PW land	PW ice	CLW ocean	CLW land	CLW ice	AVTP ocean	AVTP land	AVTP ice	LST	IST	Sea EDRs
6	0.1	9	9	9	9	9	9	9	9	9	9	9	9	9	9	0.1
10	0.1	9	9	9	9	9	9	9	9	9	9	1	9	9	9	0.1
18	0.1	0.5	0.3	0.1	9	1	0.4	9	9	9	9	9	9	1	9	0.1
23	0.1	0.7	0.3	0.1	1	0.3	0.1	9	9	9	1	9	9	0.3	9	0.1
36	0.1	0.3	0.3	1	9	1	0.5	9	9	9	9	9	9	0.5	9	0.1
50	0.1	0.2	0.3	0.3	9	1	0.3	9	9	9	0.1	0.1	0.1	0.15	0.1	9
89	0.1	0.1	0.3	1	9	0.6	0.15	9	9	9	1	9	9	9	9	9
166	0.3	9	9	9	9	0.5	0.3	9	9	9	9	9	9	9	9	9
183	0.3	0.3	0.3	0.3	9	0.7	9	9	9	9	9	9	9	9	9	9

Driver

Table 20: Interchannel accuracy by EDR and summarized.

Chan 1	Chan 2	Interchan accur requir	AVMP ocean	AVMP land	AVMP ice	PW ocean	PW land	PW ice	CLW ocean	CLW land	CLW ice	AVTP ocean	AVTP land	AVTP ice	LST	IST	Sea EDRs
6V	6H	0.04	9	9	9	9	9	9	9	9	9	9	9	9	9	9	0.04
10A	10B	0.04	9	9	9	9	9	9	9	9	9	9	9	9	9	9	0.04
18A	18B	0.04	1.8	1.8	1.4	0.6	1.8	0.2	1.8	1.8	1.8	1.8	1.8	1.8	1.8	1.8	0.04
23V	23H	0.04	0.4	0.6	1	0.4	0.2	0.2	1.8	1.8	1.8	1.8	1	1.8	1.6	1.8	0.04
36A	36B	0.04	1.2	0.4	1.8	1.8	1.8	0.4	1.8	1.8	1.8	1.8	1.8	1.8	1	1.8	0.04
89V	89H	0.2	1.4	0.8	1.8	1.8	0.3	0.2	1.8	1.8	1.8	1.8	1.8	1.8	1.8	0.6	9
50.3	52	0.18	0.4	0.4	0.3	0.4	0.3	0.3	1.8	1.8	1.8	1.8	1.8	1.8	0.18	0.24	9
183+-7	183+-3	0.24	1.6	0.24	0.6	0.6	1.8	0.6	1.8	1.8	1.8	1.8	1.8	1.8	1.8	1	9
183+-7	183+-1	0.22	0.8	0.22	0.44	1.8	1.8	1.8	1.8	1.8	1.8	1.8	1.8	1.8	1.8	1	9
6	10	0.04	9	9	9	9	9	9	9	9	9	9	9	9	9	9	0.04
10	18	0.04	19.8	19.8	19.8	19.8	19.8	19.8	19.8	19.8	19.8	1.8	1	1.8	1.8	19.8	0.04
18	23	0.04	0.14	1.8	0.12	0.6	0.3	0.14	1.8	1.8	1.8	1.8	1.8	1.8	1.8	0.3	0.04
18	36	0.04	0.34	1.8	0.14	1.8	1.8	1.8	1.8	1.8	1.8	1.8	1.8	1.8	1.8	1.8	0.04
23	36	0.04	1.2	0.3	0.38	1.2	1	0.12	1.8	1.8	1.8	1	1.8	1.8	0.44	1.8	0.04
23	183	0.1	1.8	0.16	0.38	0.6	0.32	0.1	1.8	1.8	1.8	0.6	1.8	1.8	0.22	1.8	9
36	50	0.12	0.8	0.18	0.26	0.4	0.32	0.12	1.8	1.8	1.8	1.8	1.8	1.8	0.4	0.24	9
50	89	0.18	0.2	0.7	1.8	1.8	0.32	1	1.8	1.8	1.8	0.18	0.4	0.3	0.28	0.24	9
89	166	0.2	0.24	1.8	0.5	0.6	1.8	0.2	1.8	1.8	1.8	1	0.6	1.8	0.44	0.4	9
166	183	0.2	1	0.2	0.8	1.8	0.4	0.24	1.8	1.8	1.8	1.8	1.8	1.8	0.6	1.8	9

Overrides absolute

Driver

REFERENCES

AIRS Team (Chahine, M. T., Aumann, H., Goldberg, M., McMillin, L., Rosenkranz, P., Staelin, D., Strow, L., Susskind, J., Gunson, M.), AIRS-Team Retrieval for Core Products and Geophysical Parameters – Level 2, Version 2.1, JPL D-17006, 1999.

Eyre, J.R., Inversion of cloudy satellite sounding radiances by nonlinear optimal estimation: Theory and simulations for TOVS and application to TOVS data, *Quart. J. Roy. Meteor. Soc*., **115**, pp 1001–1037, 1989a.

Eyre, J. R., Inversion of cloudy satellite sounding radiances by nonlinear optimal estimation. II: Application to TOVS data. *Q. J. R. Meteorol. Soc.*, **115**, pp 1027-1037, 1989b.

LIST OF ACRONYMS

ADD	Algorithm Description Document
AER	Atmospheric and Environment Research
AGL	Above Ground Level
AIRS	Atmospheric InfraRed Sounder
ALFA	AER Local Area Forecast Model
AMS	American Meteorological Society
AMSR	Advanced Microwave Scanning Radiometer
AMSU	Advanced Microwave Sounding Unit
APS	Algorithm Performance Simulation
ARA	Atmospheric Radiation Analysis
ARD	Algorithm Requirements Document
ARM	Atmospheric Radiation Measurement
ASRR	Algorithm System Requirements Review
ATBD	Algorithm Theoretical Basis Document
ATOVS	Advanced TOVS
AVHRR	Advanced Very High Resolution Radiometer
BT	Brightness Temperature
CC	Cloud Clearing
CEPEX	Central Equatorial Pacific Experiment
CF	Central frequency
CHARTS	Code for High resolution Accelerated Radiative Transfer with Scattering
CKD	Clough, Kneizys and Davies
CLW	Cloud Liquid Water
CMIS	Conical Microwave Imaging Sounder
COD	Cloud Optical Depth
CTH	Cloud Top Height
CTP	Cloud Top Pressure
DEM	Digital Elevation Model
DMSP	Defense Meteorological Satellite Program
DoD	Department of Defense
DOE	Department of Energy
ECMWF	European Center for Medium-range Weather Forecasts
EDR	Environmental Data Record
EIA	Earth Incidence Angle
EOF	Empirical Orthogonal Function
EOS	Earth Observing System
ESFT	Exponential Sum Fitting Technique
FFT	Fast Fourier Transform
FIRE	First ISCCP Regional Experiment
FOR	Field Of Regard
FOV	Field Of View
GPS	Global Positioning System
GSFC	Goddard Space Flight Center
HCS	Horizontal Cell Size
HIRS	High-resolution Infrared Sounder
HSB	Humidity Sounder of Brazil

HSR	Horizontal Spatial Resolution
IPO	Integrated Program Office
IPT	Integrated Product Team
ISCCP	International Satellite Cloud Climatology Project
IST	Ice Surface Temperature
IWVC	Integrated Water Vapor Content
JHU	Johns Hopkins University
JPL	Jet Propulsion Laboratory
LA	Lower Atmosphere
LAT	Latitude
LBL	Line By Line
LBLRTM	Line By Line Radiative Transfer Model
LMD	Laboratoire de Météorologie Dynamique
LON	Longitude
LOS	Line Of Sight
LST	Land Surface Temperature
L-V	Levenberg-Marquardt
LVM	Levenberg-Marquardt
MHS	Microwave Humidity Sounder
ML	Maximum Likelihood
MSU	Microwave Sounding Unit
MW	Microwave
NASA	National Aeronautics and Space Administration
NCAR	National Center for Atmospheric Research
NCEP	National Center for Environmental Prediction
NDSI	Normalized Difference Snow Index
NDVI	Normalized Difference Vegetation Index
NEDN	Noise Equivalent Difference
NESDIS	National Environmental Satellite, Data, and Information Service
NN	Neural Network
NOAA	National Oceanic and Atmospheric Administration
NPM	Numerical Prediction Model
NPOESS	National Polar-orbiting Operational Environmental satellite System
NRL	Naval Research Laboratory
NWP	Numerical Weather Prediction
OD	Optical Depth
OI	Optimal Interpolation
OLS	Operational Linescan System
OMIS	Operational Multi-Spectral Imaging Suite
OMPS	Ozone Mapping and Profiler Suite
OSS	Optimal Spectral Sampling
PCA	Principal Component Analysis
PDR	Preliminary Design Review
PSD	Power Spectral Density
POES	Polar Orbiting Environmental Satellite
Psfc	Surface Pressure
PSURF	Surface Pressure
QC	Quality Control
RDR	Raw Data Records

RH	Relative Humidity
RMS	Root Mean Square
RMSE	Root Mean Square Error
RRTM	Rapid Radiative Transfer Model
RT	Radiative Transfer
RTA	Radiative Transfer Algorithm
RTE	Radiative Transfer Equation
RTM	Radiative Transfer Model
S/N	Signal/Noise
SAR	Synthetic Aperture Radar
SDR	Sensor Data Record
SEIT	System Engineering Integrated Product Team
SFR	System Functional Review
SGI	Silicon Graphics, Inc.
SPS	System Performance Simulation
SRD	Sensor Requirement Document
SRR	System Requirements Review
SSM/I	Special Sensor Microwave/Imager
SSM/T	Special Sensor Microwave/Temperature
SSMIS	Special Sensor Microwave Imager Sounder
SST	Sea Surface Temperature
SVD	Single Value Decomposition
SW	Shortwave
T	Temperature
TBD	To Be Determined (by contractor)
TBR	To Be Resolved (by contractor/government)
TBS	To Be Supplied (by government)
TIGR	Thermodynamic Initial Guess Retrieval
TIM	Technical Interchange Meeting
TOA	Top Of Atmosphere
TOD	Time of Day
TOVS	TIROS-N Operational Vertical Sounder
TRD	Technical Requirements Document
TSKIN	Skin Temperature
UA	Upper Atmosphere
UR	Unified Retrieval
USGS	United States Geological Survey
VIIRS	Visible/Infrared Imager/Radiometer Suite
WPTB	Weather Product Test Bed
WV	Water Vapor
WVF	Water Vapor Fraction